



Published in final edited form as:

Cancer Res. 2008 September 15; 68(18): 7661–7669. doi:10.1158/0008-5472.CAN-08-1510.

## Withaferin A Causes FOXO3a- and Bim-Dependent Apoptosis and Inhibits Growth of Human Breast Cancer Cells *In Vivo*

Silvia D. Stan<sup>\*</sup>, Eun-Ryeong Hahm<sup>\*</sup>, Renaud Warin, and Shivendra V. Singh

Department of Pharmacology & Chemical Biology, and University of Pittsburgh Cancer Institute, University of Pittsburgh School of Medicine, Pittsburgh, Pennsylvania

### Abstract

Withaferin A (WA) is derived from the medicinal plant *Withania somnifera* which has been safely used for centuries in Indian Ayurvedic medicine for treatment of different ailments. We now demonstrate, for the first time, that WA exhibits significant activity against human breast cancer cells in culture and *in vivo*. The WA treatment decreased viability of MCF-7 (estrogen-responsive) and MDA-MB-231 (estrogen-independent) human breast cancer cells in a concentration-dependent manner. The WA-mediated suppression of breast cancer cell viability correlated with apoptosis induction characterized by DNA condensation, cytoplasmic histone-associated DNA fragmentation, and cleavage of poly-(ADP-ribose)-polymerase. On the other hand, a spontaneously immortalized normal mammary epithelial cell line (MCF-10A) was relatively more resistant to WA-induced apoptosis compared with breast cancer cells. The WA-mediated apoptosis was accompanied by induction of Bim-s and Bim-L in MCF-7 cells and induction of Bim-s and Bim-EL isoforms in MDA-MB-231 cells. The cytoplasmic histone-associated DNA fragmentation resulting from WA exposure was significantly attenuated by knockdown of protein levels of Bim and its transcriptional regulator FOXO3a in both cell lines. Moreover, FOXO3a knockdown conferred marked protection against WA-mediated induction of Bim-s expression. The growth of MDA-MB-231 cells implanted in female nude mice was significantly retarded by five weekly i.p. injections of 4 mg WA/kg body weight. The tumors from WA-treated mice exhibited reduced cell proliferation and increased apoptosis compared with tumors from control mice. These results point towards an important role of FOXO3a and Bim in regulation of WA-mediated apoptosis in human breast cancer cells.

### Keywords

Withaferin A; FOXO3a; Bim; Apoptosis; Breast Cancer; Chemoprevention

### Introduction

Breast cancer continues to be a leading cause of cancer-related deaths in women worldwide despite significant advances in screening techniques leading to early detection of the disease (1). The known risk factors for breast cancer include family history, Li-Fraumeni syndrome, atypical hyperplasia of the breast, late age at first full-term pregnancy, early menarche, and late menopause (2–4). Because some of these risk factors are not easily modifiable (*e.g.*, genetic predisposition), other strategies for reduction of the breast cancer risk must be considered. Even though selective estrogen-receptor (ER) modulators (*e.g.*, tamoxifen) appear promising for prevention of breast cancer, this strategy is largely ineffective against ER negative breast

Requests for reprints: Shivendra V. Singh, Ph.D., 2.32A Hillman Cancer Center Research Pavilion, 5117 Centre Avenue, Pittsburgh, PA 15213. Phone: 412-623-3263; Fax: 412-623-7828. Email: singhs@upmc.edu.

<sup>\*</sup>Equal contribution.

cancers (5,6). Moreover, selective ER modulators have serious side effects including increased risk of uterine cancer, thromboembolism, cataracts, and perimenopausal symptoms (5,6). Therefore, novel agents for prevention and treatment of human breast cancers, especially hormone-independent breast cancers, are highly desirable. Natural products have received increasing attention in recent years for the discovery of novel cancer preventive and therapeutic agents (7).

Withaferin A (WA) is a bioactive compound derived from the medicinal plant *Withania somnifera* (commonly known as ashwagandha or Indian winter cherry), which has been safely used for centuries in the Indian Ayurvedic medicine practice for the treatment of various ailments (8–13). Ashwagandha is also recommended as a tonic for overall well-being (13) and the extract of *Withania somnifera* L. is available over the counter in the United States as a dietary supplement. The known pharmacological effects of *Withania somnifera* extract include modulation of immune function (8), cardioprotection from ischemia and reperfusion injury (9), protection of 6-hydroxydopamine-induced Parkinsonism in rats (10), anti-bacterial effects (11), and anti-inflammatory effects (12). Crude ethanol extract of *Withania somnifera* suppressed lipopolysaccharide-induced production of inflammatory cytokines, including tumor necrosis factor- $\alpha$ , interleukin-1 $\beta$ , and interleukin-12 in peripheral blood mononuclear cells (14). Extract of *Withania somnifera* as well as WA potently inhibited nuclear factor- $\kappa$ B activation (15,16). The WA was shown to be a radiosensitizer and suppressor of mouse Ehrlich ascites carcinoma growth (17–20). More recent studies have demonstrated that WA suppresses growth of human cancer cells by causing apoptosis (21–23), but the mechanism of proapoptotic response to WA is poorly understood. Suppression of angiogenesis, alteration of cytoskeletal architecture, and inhibition of proteasomal activity by WA has also been documented (21,24, 25).

The present study was undertaken to determine efficacy of WA against human breast cancer cells. We demonstrate that WA exhibits significant growth inhibitory effect against MCF-7 (estrogen-responsive) and MDA-MB-231 (estrogen-independent) human breast cancer cell lines in association with apoptosis induction. The WA-mediated apoptosis in breast cancer cells is regulated by FOXO3a and its transcriptional target Bim. In addition, WA administration significantly retards growth of MDA-MB-231 cells *in vivo*, which correlates with reduced cell proliferation and increased apoptosis in the tumor mass. The results of the present study merit clinical investigation to determine efficacy of WA against human breast cancers.

## Materials and Methods

### Reagents

The WA was purchased from ChromaDex. Dimethyl sulfoxide (DMSO), 4',6-diamidino-2-phenylindole (DAPI), and cremophor-EL were purchased from Sigma-Aldrich. The cell culture media, antibiotic mixture, and fetal bovine serum were purchased from Invitrogen or Mediatech. The antibodies against Bax, Bak, Bcl-xL, Mcl-1, poly-(ADP-ribose)-polymerase (PARP), and Bim were from Santa Cruz Biotechnology; the anti-actin antibody was from Sigma; the antibodies against Bcl-2 and proliferating cell nuclear antigen (PCNA) were from DakoCytomation; and anti-FOXO3a antibody was from Upstate Biotechnology. The ApopTag Plus Peroxidase *In situ* Apoptosis detection kit was from Chemicon International-Millipore.

### Cell culture and cell viability assay

The MCF-7, MDA-MB-231, and MCF-10A cell lines were purchased from the American Type Culture Collection and maintained as described by us previously (26). The MDA-MB-231 cell line stably expressing firefly luciferase (MDA-MB-231-luc-D3H1) was purchased from Caliper Life Sciences and maintained as recommended by the provider. Each cell line was

maintained at 37°C in an atmosphere of 5% CO<sub>2</sub> and 95% air. The effect of WA treatment on viability of MCF-7 and MDA-MB-231 cells was determined by trypan blue dye exclusion assay as described by us previously (27).

### Determination of apoptosis

The proapoptotic effect of WA was assessed by fluorescence microscopy following staining the cells with DAPI and quantification of cytoplasmic histone-associated DNA fragmentation. The DAPI assay was performed essentially as described by us previously (27). Quantitation of cytoplasmic histone-associated DNA fragmentation was performed using a kit from Roche Applied Science according to the manufacturer's recommendations.

### Immunoblotting

Desired cells ( $1 \times 10^6$ ) were seeded in 100-mm culture dishes, allowed to attach by overnight incubation, and treated with DMSO (control) or 2.5 and 5.0  $\mu\text{mol/L}$  WA for specified time periods. The cell lysate was prepared as described by us previously (28). The cell lysates were cleared by centrifugation at 14,000 rpm for 30 min. The lysate proteins were resolved by 10 or 12.5% SDS-PAGE and transferred onto polyvinylidene fluoride membrane. The membrane was incubated with Tris-buffered saline containing 0.05% Tween 20 and 5% (w/v) nonfat dry milk. The membrane was then treated with the desired primary antibody for 1 h at room temperature or overnight at 4°C. Following treatment with the appropriate secondary antibody, the immunoreactive bands were visualized using the enhanced chemiluminescence method. The blots were stripped and re-probed with anti-actin antibody to normalize for differences in protein loading. Change in the level of desired protein was determined by densitometric scanning of the immunoreactive band and corrected for actin loading control. Immunoblotting for each protein was performed at least twice using independently prepared lysates to ensure reproducibility of the results.

### RNA interference

A control non-specific siRNA (UUCUCCGAACGUGUCACG UdTdT) was purchased from Qiagen. The Bim- and FOXO3a-targeted siRNAs were purchased from Santa Cruz Biotechnology (29). The sequences of the Bim- and FOXO3a-targeted siRNAs are not revealed by the manufacturer. The cells were seeded in six-well plates and transfected at 50% confluency with 200 nmol/L of control non-specific siRNA, Bim-targeted siRNA or FOXO3a-specific siRNA using OligofectAMINE according to the manufacturer's instructions. Twenty-four hours after transfection, the cells were treated with DMSO (control) or 5  $\mu\text{mol/L}$  WA for 24 h. The cells were then collected and processed for immunoblotting and analysis of cytoplasmic histone-associated DNA fragmentation.

### Xenograft studies

Eight-week old female nude (*nu/nu*) mice were purchased from Harlan Sprague-Dawley and acclimated for 1 week prior to start of the experiment. For subcutaneous xenograft study, the mice were randomized into two groups of 8 mice/group. The mice were injected intraperitoneally (i.p.) with either vehicle (10% DMSO, 40% cremophor-EL, and 50% PBS) or vehicle containing 4 mg WA/kg body weight on Monday through Friday for 2.5 weeks prior to the tumor cell injection to mimic a prevention protocol. Exponentially growing MDA-MB-231 cells were suspended in PBS and mixed in a 1:1 ratio with Matrigel. A 0.1 mL suspension containing  $2.5 \times 10^6$  cells was injected subcutaneously on both left and right flank of each mouse above the hind limb. Tumor volume and body weights were recorded as described by us previously (30–32). For the orthotopic model, eight-week old female nude mice were randomized into two groups ( $n = 5$ ) and treated i.p. with the vehicle or 4 mg WA/kg body weight on Monday through Friday for two weeks as described above. Exponentially

growing MDA-MB-231-luc-D3H1 cells ( $\sim 2.5 \times 10^6$ ) mixed with Matrigel (1:1 ratio) were injected into the mammary fat pad of each mouse. Tumor size was measured by bioluminescence imaging using a Xenogen IVIS 200 system (Caliper Life Sciences). For imaging, mice were administered i.p. with 150 mg D-luciferin/kg body weight (Caliper Life Sciences) 15 min before determination of the bioluminescence. Subsequently, the mice were anesthetized with 1–3% isoflurane and placed onto the warmed stage inside the light-tight camera box. The photons emitted by the bioluminescent tumor cells were detected by the IVIS camera system, integrated, and digitized. Regions of interest (ROI) from displayed images were identified around the tumor sites and quantified as total photon counts/s using Living Image<sup>®</sup> software (Caliper Life Sciences). A pseudocolor bioluminescent image from blue (least intense) to red (most intense) representing the spatial distribution of the detected photons emitted within the animal allowed localization and measurement of the tumor growth. Background photon flux was determined from an ROI of the same size placed in a non-luminescent area nearby and then subtracted from the measured luminescent signal intensity. All light measurements were performed under the same conditions.

### H&E staining and immunohistochemical analysis of PCNA expression

A portion of the tumor tissue removed from the control and WA-treated mice (subcutaneous xenograft study) was fixed in 10% neutral-buffered formalin, dehydrated, embedded in paraffin, and sectioned at 4–5  $\mu\text{m}$  thickness. Representative tumor sections from control and WA-treated mice were processed for H&E staining and immunohistochemical analysis of PCNA expression. Immunohistochemical analysis of PCNA expression was performed as described by us previously (32). At least three non-overlapping representative images of each tissue were captured from each section using the camera attached to the microscope. The images were analyzed using Image ProPlus 5.0 software (Media Cybernetics, Silver Spring, MD) for quantitation of PCNA expression.

### Detection of apoptotic bodies by terminal deoxynucleotidyl transferase-mediated dUTP nick-end labeling (TUNEL)

The paraffin-embedded tissue sections were deparaffinized, rehydrated, and then used to visualize apoptotic cells by TUNEL staining employing the ApopTag Plus Peroxidase *In Situ* Apoptosis kit and following the manufacturer's protocol. Apoptotic bodies in the tumor sections were quantified by counting the number of TUNEL positive cells in at least three randomly selected, non-overlapping high-power (200 $\times$  magnification) fields on each sample.

### Statistical analysis

Statistical significance of difference in measured variables between control and WA-treated groups was determined by one-way ANOVA followed by Dunnett's or Bonferroni's test or t-test. Difference was considered significant at  $P < 0.05$ .

## Results

### WA treatment decreased survival of cultured human breast cancer cells

We determined the effect of WA treatment (refer to Fig. 1A for chemical structure of WA) on viability of MCF-7 and MDA-MB-231 cells, which respectively are well-characterized representatives of estrogen-responsive and estrogen-independent human breast cancers. The MCF-7 cell line, which is estrogen receptor positive, was isolated from pleural effusion of a stage IV invasive ductal carcinoma. The MCF-7 cells are aneuploid with high chromosomal instability and defective for the G1 and mitotic spindle checkpoint but express normal p53 (reviewed in *Ref.* 33). The MDA-MB-231 cell line, which was derived from a stage IV invasive ductal carcinoma, is estrogen receptor negative, partially proficient for all cell cycle

checkpoints, and expresses mutant p53 (33). Survival of MCF-7 (Fig. 1B) and MDA-MB-231 cells (Fig. 1C) was decreased significantly after a 24-h exposure to WA in a concentration-dependent manner with an  $IC_{50}$  of  $<2 \mu\text{mol/L}$ . These results indicated that WA suppressed survival of human breast cancer cells regardless of their estrogen-responsiveness or p53 status.

### WA treatment caused apoptosis in cultured human breast cancer cells

Antiproliferative effect of many naturally-occurring cancer chemopreventive agents, including garlic-derived organosulfur compounds, cruciferous vegetable-derived isothiocyanates, and constituents of alternative and complementary medicine (*e.g.*, honokiol and guggulsterone), is tightly linked to their ability to cause apoptosis (26,27,34,35). We raised the question of whether the WA-mediated suppression of MCF-7 and MDA-MB-231 cell viability was due to apoptosis induction. We addressed this question by determining the effect of WA treatment on cytoplasmic histone-associated DNA fragmentation, which is a well-accepted technique for quantitation of apoptosis. As can be seen in Fig. 2A, WA treatment increased cytoplasmic histone-associated DNA fragmentation over DMSO-treated control in both cell lines in a concentration- and time-dependent manner. For example, the cytoplasmic histone-associated DNA fragmentation resulting from a 24-, 36- and 48-h exposure of MCF-7 cells to  $2.5 \mu\text{mol/L}$  WA was increased by about 2.1-, 7.3-, and 6.4-fold, respectively, compared with DMSO-treated control (Fig. 2A). We confirmed proapoptotic effect of WA by DAPI assay, which is another widely used technique for detection of apoptosis. The DAPI assay revealed abundance of cells with condensed and fragmented DNA in WA-treated MCF-7 and MDA-MB-231 cultures, which were rare in DMSO-treated controls (results not shown). Apoptotic cells with condensed and fragmented DNA (DAPI assay) were scored from control (DMSO-treated) and WA-treated ( $2.5$  and  $5 \mu\text{mol/L}$  WA) cultures of MCF-7 and MDA-MB-231 cells. The percentage of apoptotic cells was increased by about 25- and 30-fold upon a 24-h treatment of MDA-MB-231 cells with  $2.5$  and  $5 \mu\text{mol/L}$  WA, respectively, compared with DMSO-treated control. Consistent with these results, the WA treatment caused cleavage of PARP in MDA-MB-231 (Fig. 2B) and MCF-7 cells (results not shown). These results indicated that WA treatment caused apoptotic cell death in both MCF-7 and MDA-MB-231 cell lines.

Next, we addressed the question of whether proapoptotic effect of WA was selective towards cancer cells using a non-tumorigenic normal mammary epithelial cell line (MCF-10A). The MCF-10A cell line was isolated from fibrocystic breast disease and was spontaneously immortalized (33). The MCF-10A cells have intact cell cycle checkpoints and normal proliferation controls (33). As can be seen in Fig. 2C, the MCF-10A cell line was relatively more resistant to WA-mediated cytoplasmic histone-associated DNA fragmentation compared with MDA-MB-231 or MCF-7 cells (Fig. 2A). For example, a statistically significant increase in cytoplasmic histone-associated DNA fragmentation over DMSO-treated control in MCF-10A cells was observed at  $10 \mu\text{mol/L}$  WA concentration (Fig. 2C), whereas lower concentrations of WA were proapoptotic in MCF-7 and MDA-MB-231 cells (Fig. 2A). Collectively, these results indicated that the human breast cancer cells were relatively more sensitive to apoptosis induction by WA compared with a normal mammary epithelial cell line.

### WA treatment altered levels of Bcl-2 family proteins in breast cancer cells

The Bcl-2 family proteins play critical roles in regulation of apoptosis by functioning as either promoters (*e.g.*, Bax and Bak) or inhibitors (*e.g.*, Bcl-2 and Bcl-xL) of the cell death (36,37). To gain insight into the mechanism of WA-mediated apoptosis, we determined its effect on expression of Bcl-2 family proteins by immunoblotting (Fig. 3). The WA treatment caused a modest increase in the protein levels of Bak in both MCF-7 (Fig. 3A) and MDA-MB-231 cells (Fig. 3B) and Bax in MCF-7 cells (up to 2.7-fold increase compared with DMSO-treated control). The WA-treated MCF-7 and MDA-MB-231 cells exhibited modest induction of Bcl-2 protein levels at 6–12-h time points, especially at  $5 \mu\text{mol/L}$  concentration, followed by a decline



in its expression 24-h post-exposure (~50–90% decrease relative to DMSO-treated control). Exposure of MCF-7 and MDA-MB-231 cells to WA also resulted in induction of Bcl-xL and Mcl-1 protein levels as well as Mcl-1 cleavage to a 32 kDa intermediate in both cell lines (Fig. 3A,B). However, the most conspicuous effect of WA treatment was induction of Bim isoforms in both cells. In MCF-7 cells, the WA treatment caused a dose-dependent and marked increase in the protein levels of short and long forms of Bim (Bim-s and Bim-L, respectively; Fig. 3A). The WA-treated MDA-MB-231 cells exhibited induction of protein levels of Bim-s as well as extra-long form (Bim-EL) of the protein (Fig. 3B). Together, these results indicated that WA treatment caused an increase in the levels of both proapoptotic (Bak, Bax, and Bim) and anti-apoptotic (Bcl-2, Bcl-xL, and Mcl-1) Bcl-2 family proteins in human breast cancer cells.

### **Bim knockdown conferred protection against WA-mediated apoptosis in MCF-7 and MDA-MB-231 cells**

Because WA treatment caused a marked increase in the protein levels of Bim isoforms in both MDA-MB-231 and MCF-7 cells, we proceeded to determine their contribution to regulation of WA-induced apoptosis using siRNA technology. Transient transfection of MDA-MB-231 cells with a Bim-targeted siRNA resulted in more than 90% knockdown of Bim-EL protein (Fig. 4A, lane 2 in the *inset*) compared with cells transiently transfected with a control non-specific siRNA (Fig. 4A, lane 1 in the *inset*). The Bim-L or Bim-s isoforms were undetectable since their constitutive expression is very low in control (untreated) MDA-MB-231 cells (Fig. 3B). Consistent with the results in un-transfected MDA-MB-231 cells (Fig. 2A), a 24-h exposure of non-specific siRNA transfected MDA-MB-231 cells to 5  $\mu\text{mol/L}$  WA resulted in statistically significant increase in cytoplasmic histone-associated DNA fragmentation compared with DMSO-treated control (Fig. 4A). On the other hand, the WA-mediated increase in cytoplasmic histone-associated DNA fragmentation was not evident in MDA-MB-231 cells with knockdown of Bim-EL protein. Similarly, knockdown of Bim-EL protein level by transient transfection of MCF-7 cells with the Bim-targeted siRNA conferred partial yet significant protection against WA-mediated cytoplasmic histone-associated DNA fragmentation compared with cells transfected with a control non-specific siRNA (Fig. 4B). The protective effect of Bim-EL knockdown on WA-mediated apoptosis was relatively more pronounced in MDA-MB-231 cells (complete protection) than in the MCF-7 cell line (partial protection), which may be attributable to a greater knockdown of the Bim-EL in the former cell line compared with MCF-7 cells (compare lane 2 in the *insets* of Fig. 4A and 4B). Nonetheless, these results indicated that induction of Bim isoforms was a critical event in WA-mediated apoptosis in human breast cancer cells.

Studies have indicated that the expression of Bim is regulated by FOXO3a (also known as FKHR-L1) transcription factor (38). We designed experiments to test whether the WA-mediated induction of Bim in our model was regulated by FOXO3a. As can be seen in Fig. 4C, the protein level of FOXO3a was decreased by more than 90% upon transient transfection of MCF-7 cells with a FOXO3a-targeted siRNA as compared with the cells transfected with a control non-specific siRNA (Fig. 4C, compare lanes 1 and 2 in the *inset*). The FOXO3a protein depletion also conferred partial yet significant protection against WA-mediated cytoplasmic histone-associated DNA fragmentation when compared with MCF-7 cells transfected with the control non-specific siRNA (Fig. 4C). A similar protection against WA-mediated cytoplasmic histone-associated DNA fragmentation by knockdown of FOXO3a protein level was also observed in the MDA-MB-231 cell line (results not shown). In addition, the WA-mediated induction of Bim-s in MCF-7 cells (Fig. 4D) and MDA-MB-231 cells (results not shown) was markedly abrogated by siRNA-based knockdown of FOXO3a protein level. These results indicated that the WA-mediated induction of Bim-s in breast cancer cells was FOXO3a-dependent. Because FOXO3a knockdown did not have a noticeable effect on Bim-EL protein

level (the top band in Fig. 4D), it is reasonable to conclude that the expression of Bim-EL isoform is not regulated by FOXO3a at least in breast cancer cells.

### WA administration retarded growth of MDA-MB-231 xenografts in female nude mice

To test *in vivo* significance of the cellular observations, we determined the effect of WA administration on MDA-MB-231 xenograft growth. The dose and route of WA administration was selected from a previous study documenting *in vivo* efficacy of WA against prostate cancer cells (22). As can be seen in Fig. 5A, the average body weights of the control and WA-treated mice did not differ significantly throughout the study. Moreover, the WA-treated mice otherwise appeared healthy and did not exhibit signs of distress such as impaired movement or posture, indigestion, and areas of redness or swelling. The average tumor volume in WA-treated mice was significantly lower compared with control mice on every week of tumor measurement starting with week 6 (Fig. 5B). For example, on week 10 the average tumor volume in control mice ( $1029 \pm 164 \text{ mm}^3$ ) was approximately 1.8-fold higher compared with WA-treated mice ( $P < 0.05$ ). Consistent with tumor volume data, the average wet weight of the tumor was significantly lower in WA-treated mice compared with control mice (Fig. 5C). These results indicated that WA administration significantly inhibited MDA-MB-231 xenograft growth in female nude without causing weight loss. We also tested the efficacy of WA against MDA-MB-231-luc-D3H1 cells directly injected into the mammary fat pad of female nude mice. Bioluminescence images for representative mouse of control and WA-treated group at 12 weeks after beginning of the study are shown in Fig. 5D. The average bioluminescence signal strength obtained at 12 weeks after the start of the study for the WA-treated mice was markedly lower compared with that of control mice. Similar to the subcutaneous xenograft study (Fig. 5A), the average body weights of the control and WA-treated mice did not differ significantly in the orthotopic study (data not shown). Collectively, these results indicated that WA treatment inhibited growth of MDA-MB-231 cells subcutaneously and orthotopically implanted in female nude mice.

### WA administration decreased cell proliferation and increased apoptosis in tumors

To test whether WA-mediated inhibition of MDA-MB-231 xenograft growth *in vivo* was associated with reduced cell proliferation and/or increased apoptosis, tumor tissues from control and WA-treated mice were processed for H&E staining, immunohistochemical analysis of PCNA expression, and TUNEL assay. Data from a representative mouse of each group are shown in Fig. 6A. The H&E staining revealed a relatively higher nuclear to cytoplasmic ratio in the tumors from control mice compared with WA-treated mice. The WA-mediated reduction in cellular proliferation *in vivo* in the tumor was confirmed by immunohistochemical analysis for PCNA expression. The PCNA is a marker for cellular proliferation and is expressed in >90% of *in situ* and invasive breast carcinomas (39). The PCNA expression was about 50% lower in tumors from WA-treated mice compared with control tumors (Fig. 6B). The proapoptotic effect of WA treatment *in vivo* was visualized by TUNEL staining (Fig. 6A). The tumors from the WA-treated mice exhibited a significantly higher count of apoptotic bodies/high-power field compared with control tumors (Fig. 6C). Collectively, these results indicated that WA administration caused suppression of cellular proliferation and increased apoptosis in the tumor *in vivo*.

## Discussion

The present study demonstrates that WA treatment exhibits significant antiproliferative activity against MCF-7 and MDA-MB-231 human breast cancer cells in culture and the MDA-MB-231 cells *in vivo* implanted in female nude mice. The WA-mediated suppression of breast cancer cell growth correlates with increased apoptosis both in cultured breast cancer cells and in the tumor tissues harvested from mice. Because WA treatment suppresses growth and causes

apoptosis in both MCF-7 (estrogen-responsive) and MDA-MB-231 cells (estrogen-independent), it is reasonable to conclude that the above cellular responses to WA are not influenced by the estrogen responsiveness. Similarly, the p53 protein, which plays an important role in apoptotic response to various stimuli (40), is not necessary for WA-mediated apoptosis since this agent is able to cause cell death in wild-type p53 expressing MCF-7 cells as well as in MDA-MB-231 cells containing mutant p53. Nonetheless, it is possible that proapoptotic response to WA is intensified by the presence of wild-type p53 since the MCF-7 cell line appears relatively more sensitive to WA-induced apoptosis compared with the MDA-MB-231 cell line based on quantitation of cytoplasmic histone-associated DNA fragmentation (Fig. 2A). However, further studies are needed to systematically explore this possibility. The present study also indicates that a spontaneously immortalized and non-tumorigenic normal mammary epithelial cell line (MCF-10A) is relatively more resistant to WA-induced apoptosis compared with MCF-7 and MDA-MB-231 cells. These results are significant since selectivity towards cancer cells is a highly desirable feature of potential cancer chemopreventive and therapeutic agents.

We raised the question of whether WA treatment caused growth arrest independent of apoptosis in breast cancer cells. We have addressed this question by determining the effect of WA treatment on cell cycle distribution by flow cytometry using MDA-MB-231 and MCF-7 cells<sup>1</sup>. We found that WA exposure caused a dose-dependent G2/M phase cell cycle arrest as early as 8 h after treatment in both cell lines<sup>1</sup>. Even though significant increase in sub-diploid fraction (a measure of apoptotic cells) was not observed until 24 h after treatment, the G2/M arrest was maintained in WA-treated cells (2  $\mu\text{mol/L}$  for 24 h) even after their culture in drug-free medium for 24 h.<sup>1</sup> At the same time, a 24-h culture of WA-treated cells in drug-free medium also resulted in an increase in sub-diploid fraction. Based on these results, we conclude that a fraction of G2/M arrested cells in WA-treated cell cultures are probably driven to apoptotic cell death.

The present study reveals that the WA-mediated apoptosis in MCF-7 and MDA-MB-231 cells correlates with an increase in expression of both proapoptotic and anti-apoptotic Bcl-2 family proteins (Fig. 3). The most noticeable effect is evident on protein levels of Bim isoforms in both cell lines; although with different specificity. Bim is a BH-3 only member of the Bcl-2 family that is transcriptionally up-regulated in cells undergoing apoptosis (41–43). Three alternative splice variants of Bim have been described (44). The short form of Bim (Bim-s) potently induces apoptosis, while the apoptotic activity of the Bim-L and Bim-EL is suppressed by binding to the dynein motor complex (45). The Bim-L and Bim-EL bind to dynein light chain through a short peptide motif (DKSTQTP) that is absent in Bim-s (45). The WA treatment causes induction of Bim-L and Bim-s isoforms in MCF-7 cells and induction of Bim-EL and Bim-s variants in the MDA-MB-231 cell line. The WA-mediated induction of Bim-s is relatively more pronounced in the MCF-7 cell line than in MDA-MB-231, which could also account for relatively greater sensitivity of the former cell line to apoptosis induction by WA compared with the MDA-MB-231 cell line. The WA-mediated apoptosis in both cell lines is significantly attenuated by knockdown of Bim protein (Fig. 4A,B). The partial protection conferred by transient transfection of Bim siRNA in MCF-7 cells against WA-induced cytoplasmic histone-associated DNA fragmentation may be due to incomplete knockdown of the protein. The proapoptotic activity of Bim is regulated at multiple levels including transcriptional and posttranslational modifications (46). For example, FOXO3a has been implicated in transcriptional regulation of Bim (38). We also found that the WA-mediated induction of Bim-s, but not Bim-EL, is regulated by FOXO3a in our model since knockdown of this protein not only abrogates WA-mediated induction of Bim-s (Fig. 4D), but also protects

---

<sup>1</sup>Stan SD, Zeng Y, Singh SV. Dietary supplement constituent withaferin A causes irreversible G2-M phase cell cycle arrest in human breast cancer cells irrespective of estrogen responsiveness. Submitted for publication.



against apoptosis (Fig. 4C). Based on these results, it is reasonable to conclude that the FOXO3a-Bim pathway play an important role in regulation of WA-induced apoptosis.

Since preclinical *in vivo* efficacy testing of potential cancer therapeutic/preventive agents is a key step in their clinical development, we determined the effect of WA administration on growth of MDA-MB-231 cells subcutaneously and orthotopically implanted in female nude mice. We found that i.p. administration of WA delays growth of MDA-MB-231 xenografts in both models. Inhibition of PC-3 prostate cancer cell growth in male nude mice by WA treatment has also been observed (22). Consistent with the results of cellular studies, the WA-mediated suppression of MDA-MB-231 xenograft growth correlates with reduced cellular proliferation, as demonstrated by H&E staining and PCNA expression, and increased apoptosis as revealed by TUNEL assay. Thus, apoptosis induction is a critical mechanism in WA-mediated suppression of MDA-MB-231 cell growth *in vivo*.

In conclusion, the results of the present study demonstrate that WA treatment suppresses survival of MCF-7 and MDA-MB-231 cells in culture and retards growth of MDA-MB-231 xenografts *in vivo* in association with reduced cellular proliferation and increased apoptosis. The WA-mediated apoptosis in both cell lines is mediated, at least in part, by FOXO3a and Bim.

## Acknowledgements

The authors are grateful to Julie Arlotti, Yan Zeng, and Stanley W. Marynowski for technical assistance.

**Grant support:** USPHS grant CA129347, awarded by the National Cancer Institute.

## References

1. Jemal A, Siegel R, Ward E, et al. Cancer statistics, 2006. *CA Cancer J Clin* 2006;56:106–30. [PubMed: 16514137]
2. Kelsey JL, Gammon MD, John EM. Reproductive factors and breast cancer. *Epidemiol Rev* 1993;15:36–47. [PubMed: 8405211]
3. Hulka BS, Stark AT. Breast cancer: cause and prevention. *Lancet* 1995;346:883–7. [PubMed: 7564675]
4. Kelsey JL, Bernstein L. Epidemiology and prevention of breast cancer. *Annu Rev Pub Health* 1996;17:47–67. [PubMed: 8724215]
5. Fisher B, Costantino JP, Wickerham DL, et al. Tamoxifen for prevention of breast cancer: report of the national surgical adjuvant breast and bowel project P-1 study. *J Natl Cancer Inst* 1998;90:1371–88. [PubMed: 9747868]
6. Cuzick J, Forbes J, Edwards R, et al. First results from the International Breast Cancer Intervention study (IBIS-I): a randomized prevention trial. *Lancet* 2002;360:817–24. [PubMed: 12243915]
7. Newman DJ, Cragg GM, Snader KM. Natural products as sources of new drugs over the period 1981–2002. *J Nat Prod* 2003;66:1022–37. [PubMed: 12880330]
8. Agarwal R, Diwanay S, Patki P, Patwardhan B. Studies on immunomodulatory activity of *Withania somnifera* (Ashwagandha) extract in experimental immune inflammation. *J Ethnopharmacol* 1999;67:27–35. [PubMed: 10616957]
9. Gupta SK, Mohanty I, Talwar KK, et al. Cardioprotection from ischemia and reperfusion injury by *Withania somnifera*: a hemodynamic, biochemical and histopathological assessment. *Mol Cell Biochem* 2004;260:39–47. [PubMed: 15228084]
10. Ahmad M, Saleem S, Ahmad As, et al. Neuroprotective effects of *Withania somnifera* on 6-hydroxydopamine induced Parkinsonism in rats. *Hum Exp Toxicol* 2005;24:137–47. [PubMed: 15901053]
11. Owais M, Sharad KS, Shehbaz A, Saleemuddin M. Antibacterial efficacy of *Withania somnifera* (Ashwagandha) an indigenous medicinal plant against experimental murine salmonellosis. *Phytomed* 2005;12:229–35.

12. Rasool M, Varalakshmi P. Immunomodulatory role of *Withania somnifera* root powder on experimental induced inflammation: An in vivo and in vitro study. *Vascul Pharmacol* 2006;44:406–10. [PubMed: 16713367]
13. Mishra LC, Singh BB, Dagenais S. Scientific basis for the therapeutic use of *Withania somnifera* (ashwagandha): a review. *Altern Med Rev* 2000;5:334–46. [PubMed: 10956379]
14. Singh D, Aggarwal A, Maurya R, Naik S. *Withania somnifera* inhibits NF- $\kappa$ B and AP-1 transcription factors in human peripheral blood and synovial fluid mononuclear cells. *Phytother Res* 2007;21:905–13. [PubMed: 17562568]
15. Ichikawa H, Takada Y, Shishodia S, Jayaprakasam B, Nair MG, Aggarwal BB. Withanolides potentiate apoptosis, inhibit invasion, and abolish osteoclastogenesis through suppression of nuclear factor- $\kappa$ B (NF- $\kappa$ B) activation and NF- $\kappa$ B-regulated gene expression. *Mol Cancer Ther* 2006;5:1434–45. [PubMed: 16818501]
16. Kaileh M, Vanden Berghe W, Heyerick A, et al. Withaferin A strongly elicits IkappaB kinase beta hyperphosphorylation concomitant with potent inhibition of its kinase activity. *J Biol Chem* 2007;282:4253–64. [PubMed: 17150968]
17. Devi PU, Akagi K, Ostapenko V, Tanaka Y, Sugahara T. Withaferin A: a new radiosensitizer from the Indian medicinal plant *Withania somnifera*. *Int J Radiat Biol* 1996;69:193–7. [PubMed: 8609455]
18. Devi PU, Kamath R, Rao BS. Radiosensitization of a mouse melanoma by withaferin A: *in vivo* studies. *Indian J Exp Biol* 2000;38:432–7. [PubMed: 11272405]
19. Devi PU, Sharada AC, Solomon FE. *In vivo* growth inhibitory and radiosensitizing effects of withaferin A on mouse Ehrlich ascites carcinoma. *Cancer Lett* 1995;95:189–93. [PubMed: 7656229]
20. Devi PU, Sharada AC, Solomon FE, Kamath MS. *In vivo* growth inhibitory effect of *Withania somnifera* (Ashwagandha) on a transplantable mouse tumor, sarcoma 180. *Indian J Exp Biol* 1992;30:169–72. [PubMed: 1512021]
21. Yang H, Shi G, Dou QP. The tumor proteasome is a primary target for the natural anticancer compound withaferin A isolated from “Indian winter cherry”. *Mol Pharmacol* 2007;71:426–37. [PubMed: 17093135]
22. Srinivasan S, Ranga RS, Burikhanov R, Han SS, Chendil D. Par-4-dependent apoptosis by the dietary compound withaferin A in prostate cancer cells. *Cancer Res* 2007;67:246–53. [PubMed: 17185378]
23. Malik F, Kumar A, Bhushan S, et al. Reactive oxygen species generation and mitochondrial dysfunction in the apoptotic cell death of human myeloid leukemia HL-60 cells by a dietary compound withaferin A with concomitant protection by N-acetyl cysteine. *Apoptosis* 2007;12:2115–33. [PubMed: 17874299]
24. Mohan R, Hammers HJ, Bargagna-Mohan P, et al. Withaferin A is a potent inhibitor of angiogenesis. *Angiogenesis* 2004;7:115–22. [PubMed: 15516832]
25. Falsey RR, Marron MT, Gunaherath GM, et al. Actin microfilament aggregation induced by withaferin A is mediated by annexin II. *Nat Chem Biol* 2006;2:33–8. [PubMed: 16408090]
26. Xiao D, Vogel V, Singh SV. Benzyl isothiocyanate-induced apoptosis in human breast cancer cells is initiated by reactive oxygen species and regulated by Bax and Bak. *Mol Cancer Ther* 2006;5:2931–45. [PubMed: 17121941]
27. Xiao D, Choi S, Johnson DE, et al. Diallyl trisulfide-induced apoptosis in human prostate cancer cells involves c-Jun N-terminal kinase and extracellular-signal regulated kinase-mediated phosphorylation of Bcl-2. *Oncogene* 2004;23:5594–606. [PubMed: 15184882]
28. Xiao D, Srivastava SK, Lew KL, et al. Allyl isothiocyanate, a constituent of cruciferous vegetables, inhibits proliferation of human prostate cancer cells by causing G<sub>2</sub>/M arrest and inducing apoptosis. *Carcinogenesis* 2003;24:891–7. [PubMed: 12771033]
29. Chen K, Tu Y, Zhang Y, Blair HC, Zhang L, Wu C. PINCH-1 regulates the ERK-Bim pathway and contributes to apoptosis resistance in cancer cells. *J Biol Chem* 2008;283:2508–17. [PubMed: 18063582]
30. Singh AV, Xiao D, Lew KL, Dhir R, Singh SV. Sulforaphane induces caspase-mediated apoptosis in cultured PC-3 human prostate cancer cells and retards growth of PC-3 xenografts *in vivo*. *Carcinogenesis* 2004;25:83–90. [PubMed: 14514658]

31. Xiao D, Lew KL, Kim Y, et al. Diallyl trisulfide suppresses growth of PC-3 human prostate cancer xenograft *in vivo* in association with induction of multidomain proapoptotic proteins Bax and Bak. *Clin Cancer Res* 2006;12:6836–43. [PubMed: 17121905]
32. Hahm ER, Arlotti JA, Marynowski SW, Singh SV. Honokiol, a constituent of oriental medicinal herb *Magnolia officinalis*, inhibits growth of PC-3 xenografts *in vivo* in association with apoptosis induction. *Clin Cancer Res* 2008;14:1248–57. [PubMed: 18281560]
33. Morse DL, Gray H, Payne CM, Gillies RJ. Docetaxel induces cell death through mitotic catastrophe in human breast cancer cells. *Mol Cancer Ther* 2005;4:1495–504. [PubMed: 16227398]
34. Choi S, Singh SV. Bax and Bak are required for apoptosis induction by sulforaphane, a cruciferous vegetable derived cancer chemopreventive agent. *Cancer Res* 2005;65:2035–43. [PubMed: 15753404]
35. Singh SV, Choi S, Zeng Y, Hahm E, Xiao D. Guggulsterone-induced apoptosis in human prostate cancer cells is caused by reactive oxygen intermediate-dependent activation of c-Jun NH<sub>2</sub>-terminal kinase. *Cancer Res* 2007;67:7439–49. [PubMed: 17671214]
36. Chao DT, Korsmeyer SJ. Bcl-2 family: regulators of cell death. *Annu Rev Immunol* 1998;16:395–419. [PubMed: 9597135]
37. Adams JM, Cory S. The Bcl-2 protein family: arbiters of cell survival. *Science* 1998;281:1322–6. [PubMed: 9735050]
38. Dijkers PF, Medema RH, Lammers JJ, Koenderman L, Coffey PJ. Expression of the pro-apoptotic Bcl-2 family member Bim is regulated by the forkhead transcription factor FKHR-L1. *Curr Biol* 2000;10:1201–4. [PubMed: 11050388]
39. Terry G, Ho L, Londesborough P, Duggan C, Hanby A, Cuzick. The expression of FHIT, PCNA and EGFR in benign and malignant breast lesions. *Br J Cancer* 2007;96:110–7. [PubMed: 17164758]
40. Sheikh MS, Fornace AJ. Role of p53 family members in apoptosis. *J Cell Physiol* 2000;182:171–81. [PubMed: 10623880]
41. Harris CA, Johnson EM Jr. BH3-only Bcl-2 family members are coordinately regulated by the JNK pathway and require Bax to induce apoptosis in neurons. *J Biol Chem* 2001;276:37754–60. [PubMed: 11495903]
42. Putcha GV, Moulder KL, Golden JP, et al. Induction of BIM, a proapoptotic BH3-only BCL-2 family member, is critical for neuronal apoptosis. *Neuron* 2001;29:615–28. [PubMed: 11301022]
43. Whitfield J, Neame SJ, Paquet L, Bernard O, Ham J. Dominant-negative c-Jun promotes neuronal survival by reducing BIM expression and inhibiting mitochondrial cytochrome c release. *Neuron* 2001;29:629–43. [PubMed: 11301023]
44. O'Reilly LA, Cullen L, Visvader J, et al. The proapoptotic BH3-only protein bim is expressed in hematopoietic, epithelial, neuronal, and germ cells. *Am J Pathol* 2000;157:449–61. [PubMed: 10934149]
45. Puthalakath H, Huang DC, O'Reilly LA, King SM, Strasser A. The proapoptotic activity of the Bcl-2 family member Bim is regulated by interaction with the dynein motor complex. *Mol Cell* 1999;3:287–96. [PubMed: 10198631]
46. Putcha GV, Le S, Frank S, et al. JNK-mediated BIM phosphorylation potentiates BAX-dependent apoptosis. *Neuron* 2003;38:899–14. [PubMed: 12818176]

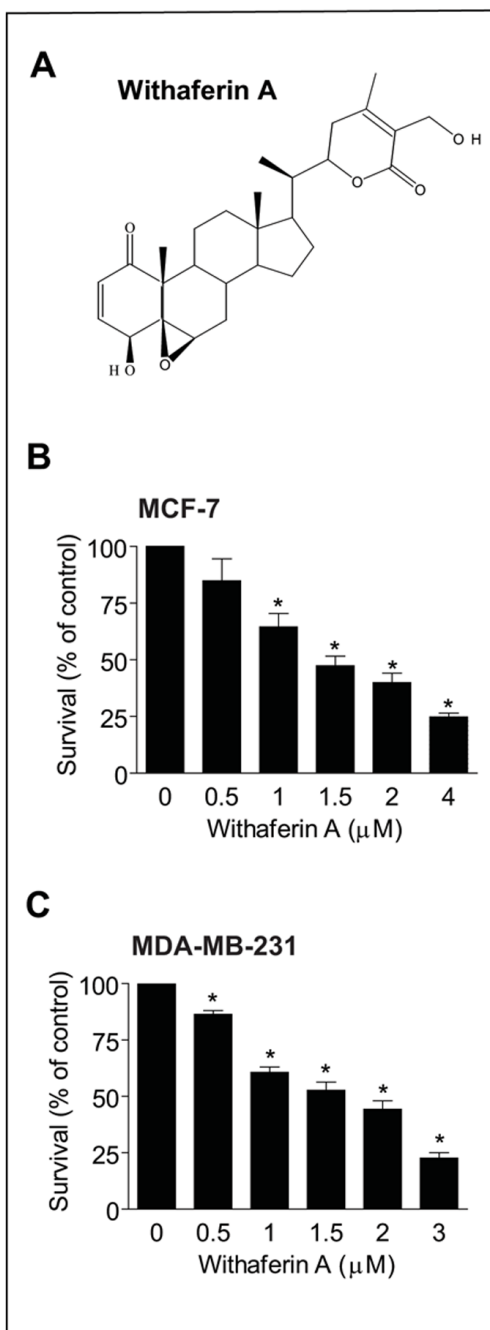


**Fig. 1.** A, chemical structure of withaferin A (WA). B, effect of WA treatment on viability of MCF-7 cells as determined by trypan blue dye exclusion assay. C, effect of WA treatment on viability of MDA-MB-231 cells as determined by trypan blue dye exclusion assay. The cells were treated with DMSO (control) or the indicated concentrations of WA for 24 h. Columns, mean (n=3); bars, SE. \*,  $P < 0.05$ , significantly different compared with control by one-way ANOVA followed by Dunnett's test. Experiments were repeated with similar results.

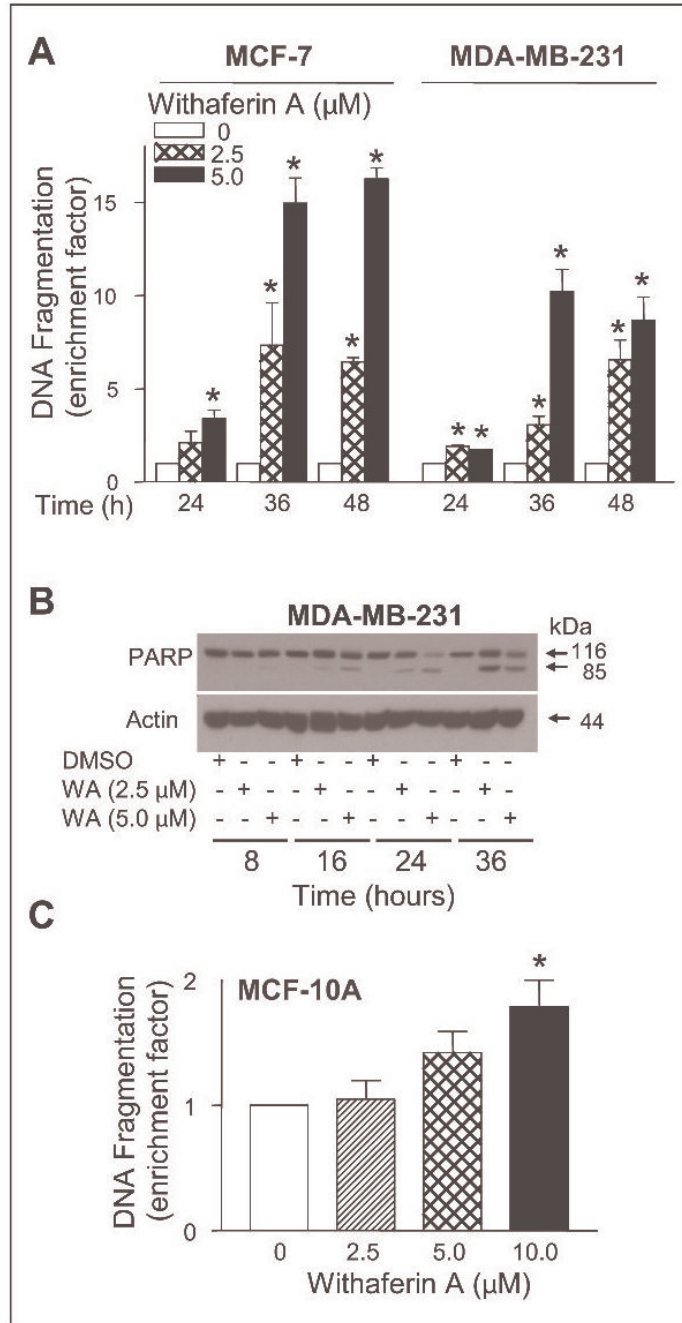


**Fig. 2.** *A*, quantitation of cytoplasmic histone-associated DNA fragmentation in MCF-7 and MDA-MB-231 cells following 24-, 36- or 48-h exposure to DMSO (control) or 2.5 and 5.0 μmol/L WA. DNA fragmentation enrichment factor relative to corresponding DMSO control is shown. *B*, immunoblotting for PARP using lysates from MDA-MB-231 cells treated for 8, 16, 24 or 36 h with DMSO (control) or the indicated concentrations of WA. The blot was stripped and re-probed with anti-actin antibody to ensure equal protein loading. *C*, quantitation of cytoplasmic histone-associated DNA fragments in MCF-10A cells following a 24-h exposure to DMSO (control) or the indicated concentrations of WA. *Columns*, mean (n=3); *bars*, SE; \*,



$P < 0.05$ , significantly different compared with DMSO-treated control by one-way ANOVA followed by Dunnett's test. Similar results were observed in replicate experiments.

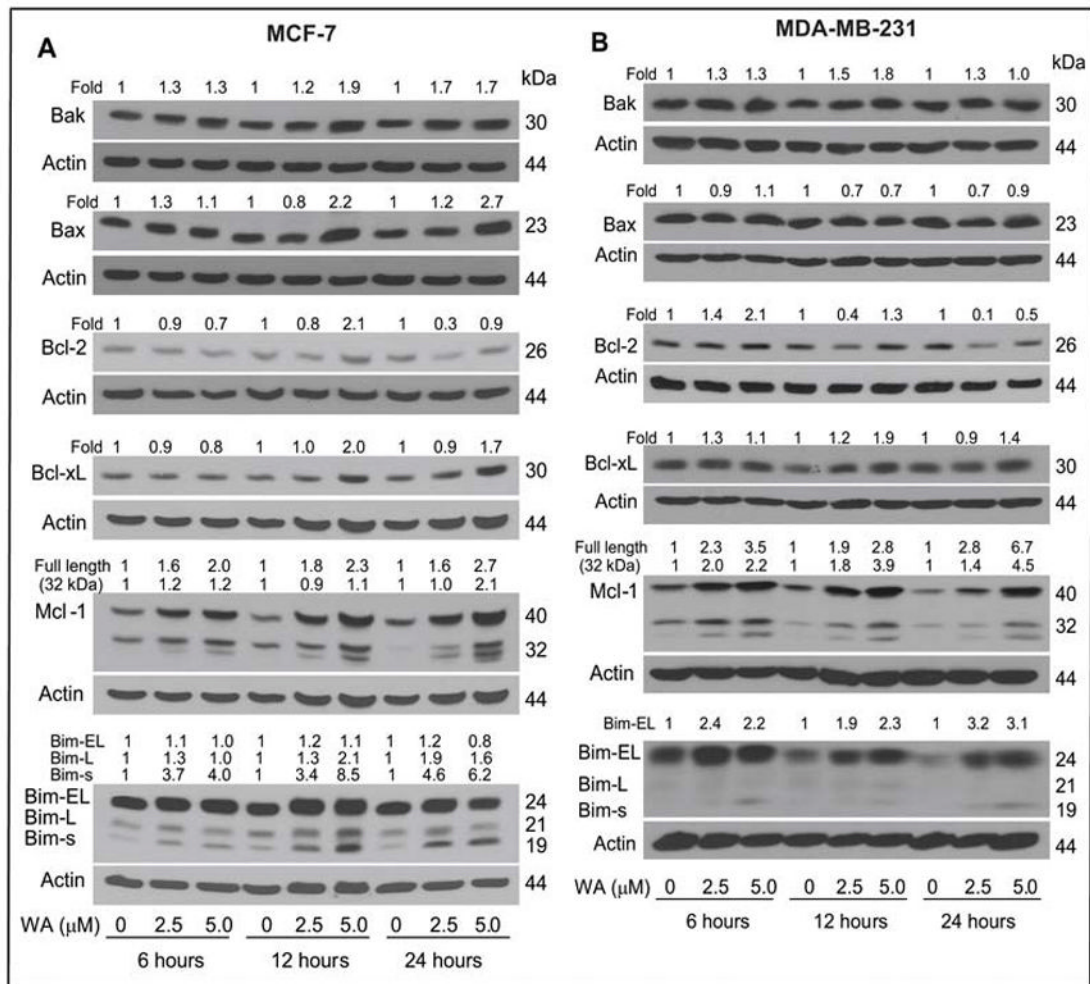


**Fig. 3.** Immunoblotting for Bcl-2 family proteins using lysates from (A) MCF-7 cells and (B) MDA-MB-231 cells treated for 6, 12 or 24 h with DMSO (control) or the indicated concentrations of WA. The blots were stripped and re-probed with anti-actin antibody to correct for differences in protein loading. Changes in protein levels after correction for actin loading control are shown on top of the immunoreactive bands.

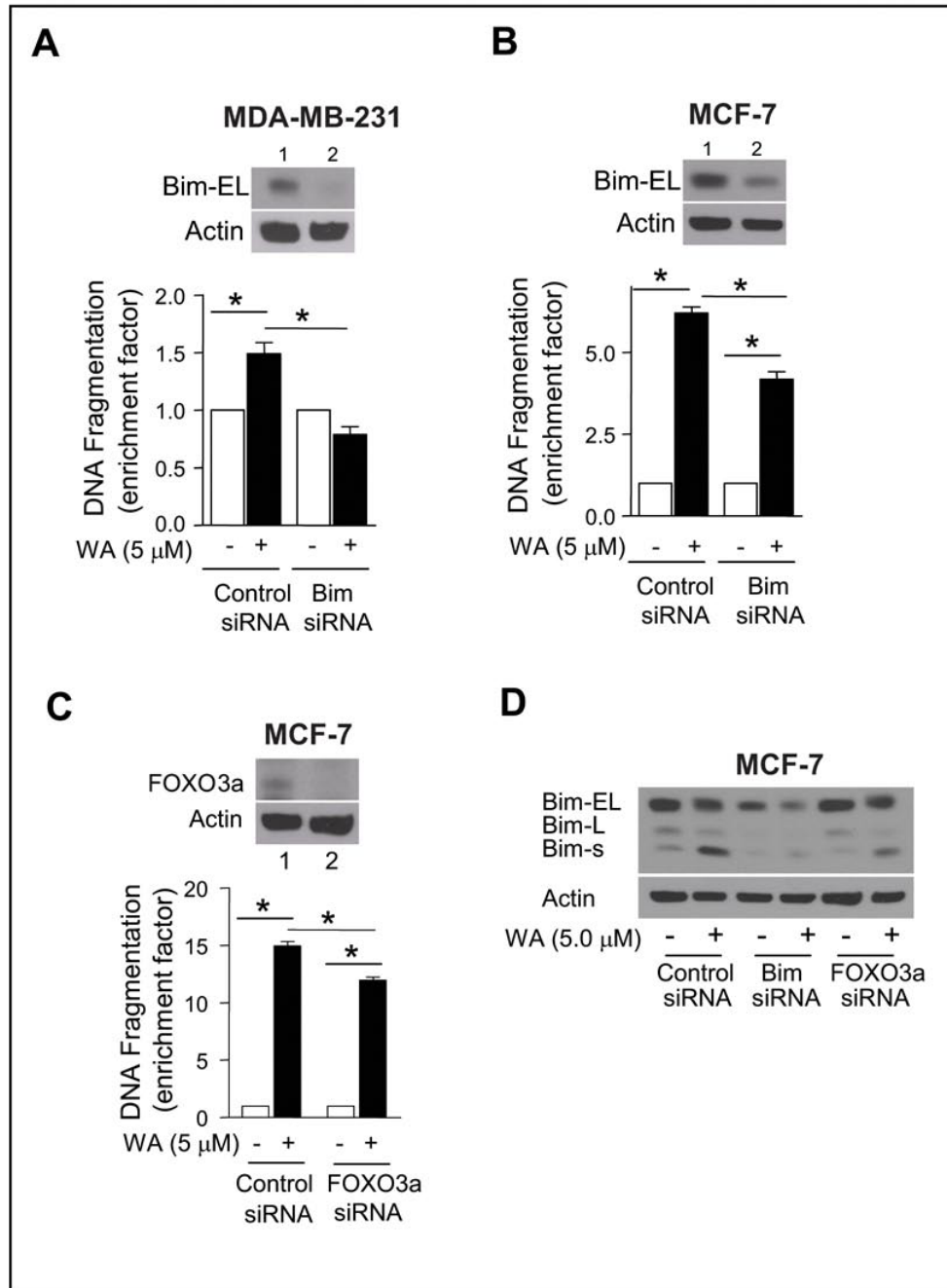


**Fig. 4.** A, cytoplasmic histone-associated DNA fragmentation in (A) MDA-MB-231 and (B) MCF-7 cells transiently transfected with a control non-specific siRNA or a Bim-targeted siRNA and treated for 24 h with either DMSO (control) or 5  $\mu$ mol/L WA. Lanes 1 and 2 in the *inset* show immunoblotting for Bim-EL in (A) MDA-MB-231 or (B) MCF-7 cells transiently transfected with the non-specific siRNA and the Bim-targeted siRNA, respectively. C, cytoplasmic histone-associated DNA fragmentation in MCF-7 cells transiently transfected with a control non-specific siRNA or a FOXO3a-targeted siRNA and treated for 24 h with either DMSO (control) or 5  $\mu$ mol/L WA. The *inset* shows immunoblotting for FOXO3a in MCF-7 cells transiently transfected with the non-specific siRNA (lane 1) and the FOXO3a-targeted siRNA

(lane 2). *Columns*, mean (n=3); *bars*, SE; \*,  $P < 0.05$ , significantly different between the indicated groups by one-way ANOVA followed by Bonferroni's multiple comparison test. *D*, immunoblotting for Bim isoforms using lysates from MCF-7 cells transiently transfected with a control non-specific siRNA, Bim-targeted siRNA, and FOXO3a specific siRNA and treated for 24 h with either DMSO (control) or 5  $\mu\text{mol/L}$  WA. The blots were stripped and re-probed with anti-actin antibody to ensure equal protein loading. The results were consistent in replicate experiments.

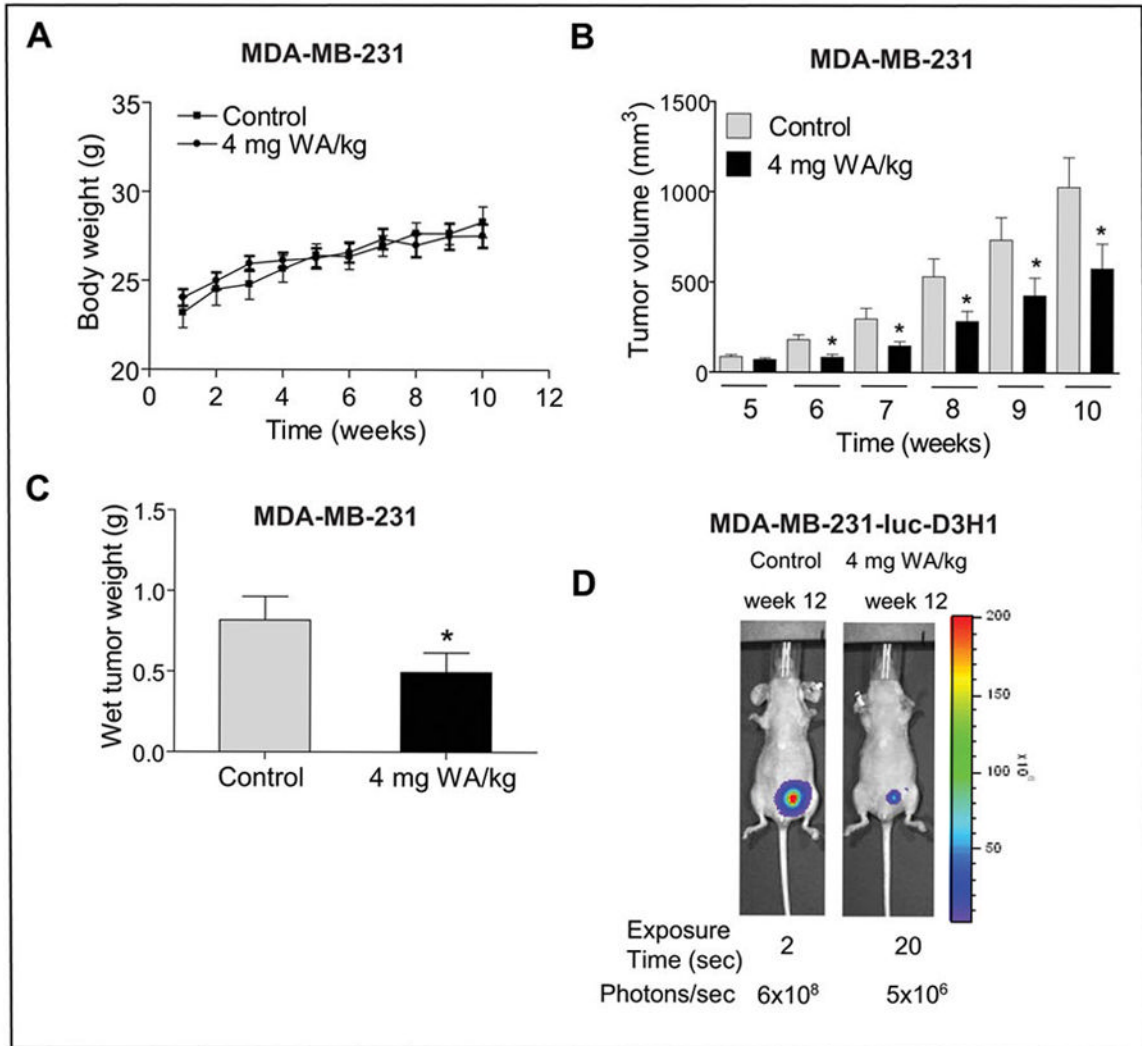


**Fig. 5.** Effect of WA administration on growth of MDA-MB-231 cells subcutaneously or orthotopically implanted in female nude mice. *A*, average body weights of the control and 4 mg WA/kg-treated mice. The body weights of the control and WA-treated mice did not differ significantly throughout the study. *B*, average tumor volume in vehicle-treated control mice and 4 mg WA/kg-treated mice. *C*, average wet tumor weight in vehicle-treated control mice and 4 mg WA/kg-treated mice. Columns, mean (control, n=12; WA, n=15); bars, SE. Even though we started with 8 mice/group with tumor cells implanted on both left and right flank of each mouse, the tumor did not grow on either side in 2 control mice and on one side in one mouse of WA treatment group. These mice were excluded from the analysis. \* $P < 0.05$ , significantly different compared with control by t-test. *D*, bioluminescence imaging at 12 weeks after the start of the study in a representative control mouse and a representative WA-treated mouse orthotopically implanted with MDA-MB-231-luc-D3H1 cells. The exposure time and photons emitted are shown.



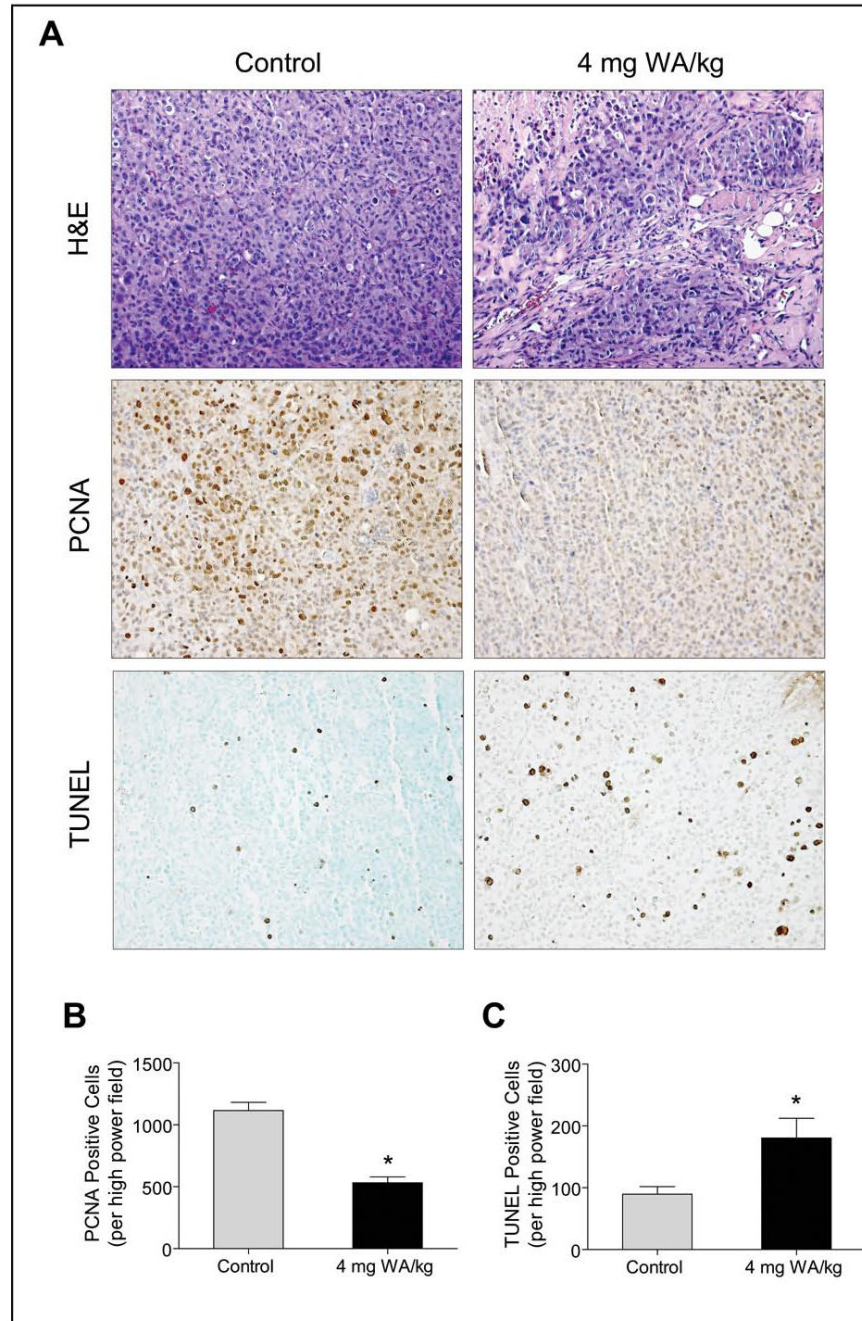


**Fig. 6.** A, histological analysis of MDA-MB-231 tumors from control and WA-treated mice (subcutaneous xenograft study) for H&E staining, proliferating cell nuclear antigen (PCNA) expression, and TUNEL positive apoptotic bodies. Representative H&E, PCNA, and TUNEL staining in tumor sections of a control and a WA-treated mouse are shown. B, quantitation of PCNA expression in tumors from control and WA-treated mice. C, quantitation of apoptotic bodies/high-power field in tumors from control and WA-treated mice. At least three randomly selected fields on each slide from tumors of five individual mouse of control and WA-treated groups were scored for PCNA expression and TUNEL positive cells. Columns, mean (n= 5), bars, SE. \* $P < 0.05$ , significantly different compared with control by t-test.